ORIGINAL



Flow boiling heat transfer capabilities of R134a low GWP substitutes inside a 4 mm id horizontal smooth tube: R600a and R152a

Giovanni A. Longo 1 · Simone Mancin 1 D · Giulia Righetti 1 · Claudio Zilio 1

Received: 4 June 2020 / Accepted: 26 October 2020 © The Author(s) 2020

Abstract

R134a was recognized as probably one of the most important refrigerants of the two past decades. Among the proposed alternative fluids, there are certainly isobutane (R600a) and R152a. This article presents about 200 new heat transfer coefficient and pressure drop data obtained during flow boiling of R152a and R600a inside a smooth copper tube having an internal diameter of 4 mm. Three saturation temperatures were considered for each refrigerant, from 5 °C to 20 °C. Furthermore, for each temperature studied, the heat flux was varied between 15 and 30 kW m⁻² and the refrigerant mass flux from 100 to 400 kg m⁻² s⁻¹. After presenting the new data, a critical comparison was proposed between the performance of these refrigerants and R134a. Finally, some classic correlations available in the literature have been implemented. The deviations between the calculated and experimental values were reported and commented.

Keywords R600a · R152a · R134a · Flow boiling · Heat transfer coefficient · Pressure drop · Low GWP refrigerant

Nomenclature

| \boldsymbol{A} | heat transfer area (m ²) |
|------------------|--|
| c_p | specific heat (J kg ⁻¹ K ⁻¹) |
| \dot{G} | refrigerant mass flux (kg m ⁻² s ⁻¹) |
| HTC | heat transfer coefficient (W m ⁻² K ⁻¹) |
| k | thermal conductivity (W m ⁻¹ K ⁻¹) |
| p | pressure (Pa) |

Highlights •About 200 new experimental data of in-tube boiling heat transfer and pressure drop of R600a and R152a are presented •R600a and R152a are investigated as low GWP alternatives of R134a

 The heat transfer coefficients and the friction loss are critically analyzed
 Some models available in the literature are used to assess the quality of the new experimental data

Simone Mancin simone.mancin@unipd.it

Giovanni A. Longo tony@gest.unipd.it

Giulia Righetti giulia.righetti@unipd.it

Claudio Zilio claudio.zilio@unipd.it

Published online: 23 November 2020

Department of Management and Engineering, University of Padova, Str.lla S. Nicola nr 3, I-36100 Vicenza, Italy

Q heat flow rate (W) q heat flux (W m⁻²)

J specific enthalpy (J kg⁻¹)

m mass flow rate (kg s⁻¹)

r latent heat (J kg $^{-1}$) t temperature (°C)

TC thermocouple

v specific volume (m³ kg⁻¹)

x vapor quality (-)

Greek

 Δ difference (-)

 μ viscosity (mPa s⁻¹)

 ρ density (kg m⁻³)

 σ surface tension (N m⁻¹)

Subscript

a acceleration

c local

crit critical

f frictional

in inlet

L liquid

out outlet

pre pre-evaporator

red reduced

ref refrigerant

sat saturation



sub subcooled tot total V vapor w water

1 Introduction

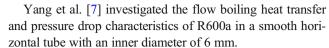
Following the environmental issues linked to anthropogenic greenhouse effect and the consequent increment of ambient temperatures, several HFC refrigerants, including R134a, are subjected to a progressive phase-down, depending on local legislations.

In the last years, several low-GWP (Global Warming Potential) synthetic molecules, like R1234yf and R1234ze (E), have been proposed (mostly HydroFluoOlefins, HFO) as R134a replacements in some applications like mobile air conditioning and large chillers. However, since the nineties, some traditional low-GWP molecules, like R152a (an HFC) and isobutane (R600a) have been evaluated and in some cases already used as substitutes of R134a in applications like domestic appliances, heat pumps, cabin heating and cooling for vehicles [1–3].

Despite those fluids are promising alternatives to R134a and available for relatively longtime, the studies about heat transfer behavior of R152a and R600a during in-tube flow boiling are still limited. In 2019 Fang et al. [4] performed a thoroughly literature review about saturated flow boiling heat transfer. Considering horizontal smooth tubes, they found only four papers investigating R600a for a total number of 820 data points.

De Oliveira et al. [5] studied the local heat transfer coefficient and the flow pattern during flow boiling inside a 1 mm horizontal tube. The Authors demonstrated that the heat transfer coefficient was highly dependent on the mass velocity while heat flux was found to have no significant effect. Convective boiling was found to be predominant. While, nucleate boiling was predominant only at low vapor quality. In any case, the heat transfer coefficient increased with the increase of vapor quality.

Copetti et al. [6] investigated the R600a boiling heat transfer characteristics in a 2.6 mm tube and compared them against R134a ones. The Authors found that in the low quality region, there was a significant influence of heat flux on the heat transfer coefficient. While, in the high vapor quality region, for high mass velocities, that influence tended to disappear. Furthermore, they detected an influence of mass velocity on the heat transfer coefficient in most of the tests. While for the highest heat flux value, the heat transfer coefficient did not depend of mass velocity. When the Authors compared R600a and R134a observed a similar behavior.



They observed that the heat transfer coefficient was nearly independent of the mass flux in low vapor quality, while it increased with mass flux in the high vapor quality region. Then, the heat transfer coefficient increased with the heat flux in low vapor quality region. But, that increasing tendency was suppressed in the high vapor quality region.

Qiu et al. [8] collected and analyzed some saturated flow boiling heat transfer coefficients and frictional pressure drops data of R1234ze(E), R600a, and L-41b inside an 8 mm inner diameter horizontal tube.

The Authors observed that the heat transfer coefficients showed the same trend with vapor quality for each fluid. The heat transfer coefficient strongly increased with the mass flux and slightly increased with the heat flux. Then, the mass flux had a strong effect on the frictional pressure drops, but the heat flux did not show any significant influence on the frictional pressure drops The comparison between refrigerant showed that the heat transfer coefficients of R1234ze(E) were on average 33% lower than those of R600a. While the frictional pressure drops of R1234ze(E) were some 21% lower than those of R600a.

Other isobutane data were presented by Sempertegui Tapia and Ribatski [9]. In this paper the Authors presented some new R134a, R1234yf, R1234ze(E) data, including 1315 data of R600a flow boiling in a circular channel with internal diameter of 1.1 mm with mass fluxes from 200 to $500 \text{ kg m}^{-2} \text{ s}^{-1}$, heat fluxes from 15 to 145 kW m⁻², saturation temperatures of 31 and 41 °C. They concluded that in the experimental conditions where the nucleate boiling effects were predominant, the HTC increased with increasing heat flux and it was almost independent of the mass velocity. On the other hand, under experimental conditions where the convective effects were predominant, the HTC was independent of the heat flux and it increased when increasing the mass velocity. Comparing the heat transfer performance of the investigated refrigerants, it was observed that the HTC for R600a is lower than the HTC of the fluids R1234a, R1234ze(E) and R1234yf for vapor qualities lower than 0.2. However, the HTC for R600a increased drastically with increasing vapor quality reaching values up to 120% higher than the other fluids.

Again with reference to horizontal smooth tubes, only three sets of data with R152a were retrieved. The paper of Hamdar et al. [10] included 50 data points during flow boiling inside 1 mm tube, at one saturation temperature (25.2 °C), mass fluxes 210-580 kg m⁻² s⁻¹, and heat fluxes 18.5-57.5 kW m⁻².

The Authors stated that the heat transfer coefficient was dominated by nucleate boiling regime in the range of the investigated parameters.



Anwar et al. [11] collected some experimental data of R152a under upward flow boiling conditions inside a 1.6 circular tube in a vertical position. The Authors compared the R152a heat transfer coefficients and the frictional pressure drops against the R134a ones revealing a similar behavior.

The heat transfer was strongly controlled by the applied heat flux for the whole span of tests up to vapor quality of about 0.90, with insignificant contributions from mass flux and vapor quality. While, the heat transfer coefficients increased with increasing saturation temperature.

Finally, some older R152a measurements can be retrieved in the report of Ross [8], inside a 9 mm smooth tube, with mass fluxes $200-700 \text{ kg m}^{-2} \text{ s}^{-1}$, and heat fluxes $10-40 \text{ kW m}^{-2}$.

All the above reviewed papers are summarized in Table 1, where the main operating conditions are also listed.

It can be observed that the inner diameters investigated in the open literature are devoted mostly to mini tubes (ID \leq 3 mm) or to macro tubes (ID \geq 6 mm), while in the recent years there has been an increasing interest in the industry for "compact" or "small" copper tubes having 3 mm < ID <6 mm.

In fact, in the seek for refrigerant charge reduction, 4 mm tube is a new target especially for air finned coil heat exchangers [13].

In this scenario, there is surely need for further experimental investigations during flow boiling of R152a and R600a inside "compact" tubes, in order to assess the suitability of available heat transfer coefficient and pressure drop models, that have been developed with few data relative to these refrigerants and even less data collected in 3 to 6 mm diameter tubes.

Hence, this paper presents new sets of heat transfer coefficient and pressure drop measurements during flow boiling of isobutane and R152a inside a 4 mm inner diameter tube at 5, 10, 15, 20 °C saturation temperatures with mass fluxes from 100 to $400 \text{ kg m}^{-2} \text{ s}^{-1}$, and heat fluxes between 15, 20, 25 and 30 kW m^{-2} , at different vapor qualities. The new data points are compared with the measurements run with R134a in the same rig [14]. An assessment of the new data with several

models available in the literature is finally carried out in order to exploit the most suitable models for the design of evaporators using "compact" tubes.

2 Experimental set up and test procedure

The experimental set up used to collect the data here presented was designed and built to investigate both condensation and vaporization process of refrigerants inside a double tube heat exchanger, where the refrigerant flows in the inner tube and water flows in countercurrent in the annulus. It has been used to collect a large database of experimental data, under several working conditions and to investigate several refrigerants. The rig was designed in order to adjust and set the refrigerant conditions at the inlet of the copper tube placed horizontally. This tube, has an internal diameter of 4 mm and a total length of 1300 mm. It is subdivided into an 800 mm test section, and a 500 mm pre-section, used to assure a fully developed refrigerant flow regime. Furthermore, the flow rate and temperature of the water flowing in the annulus are controlled to obtain the desired heat flow rate in the test section.

Figure 1 shows a schematic of the system. It depicts the loop where the refrigerant flows, pumped by means of a variable speed volumetric pump that counteracts the pressure drops. In addition, there is a hot water loop serving the measuring section, providing the required heat flow rate. The energy balance discrepancy between the water in the hot loop and phase-changing refrigerant was always less than 2%.

There is also a second hot water loop to pre-evaporate the refrigerant to the desired inlet conditions. Finally, there is a cold water loop (water and glycol) which allows the refrigerant to condense and to be sub-cooled at the exit of the test section. The positions of the measuring instruments are also shown in the same Fig. 1. T-type thermocouples connected to a K170 Ice Point Reference, with stability of ± 0.005 °C and accuracy of ± 0.005 °C were used to measure the temperature, a Coriolis effect mass flow meter was used to measure the refrigerant flow rate and a strain-gage differential and absolute

 Table 1
 Summary of the experimental data available in the literature

| Reference | Refrigerant | Tube diameter (mm) | $G (\text{kg m}^{-2} \text{ s}^{-1})$ | $q \text{ (kW m}^{-2}\text{)}$ | t _{sat} (°C) |
|------------------------------------|-------------|--------------------|---------------------------------------|--------------------------------|-----------------------|
| De Oliveira et al. [5] | R600a | 1 | 240 to 480 | 5 to 60 | 25 |
| Copetti et al. [6] | R600a | 2.6 | 240 to 440 | 44 to 95 | 22 |
| Yang et al. [7] | R600a | 6 | 67 to 194 | 10.6 to 75 | 9.2 to 30.9 |
| Qiu et al. [8] | R600a | 8 | 200 to 400 | 5 to 10 | 20 |
| Sempertegui Tapia and Ribatski [9] | R600a | 1.1 | 200 to 500 | 15 to 145 | 31 and 41 |
| Hamdar et al. [10] | R152a | 1 | 210 to 580 | 18.5 to 57.5 | 25.2 |
| Anwar et al. [11] | R152a | 1.6 | 100-500 | 5 to 245 | 27 and 32 |
| Ross [12] | R152a | 9 | 200 to 700 | 10 to 40 | |



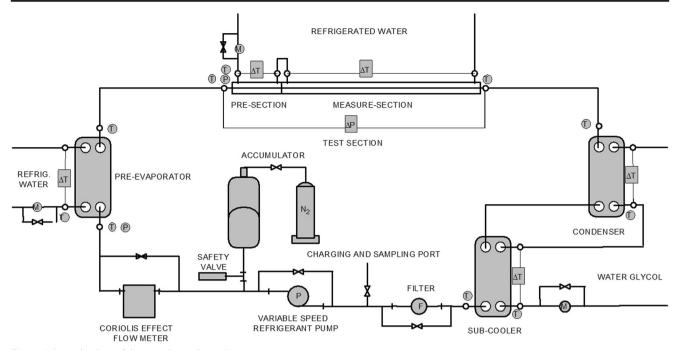


Fig. 1 Schematic view of the experimental test rig

pressure transducers measured the differential pressure drops and the total pressure. The water flow rates flowing in the auxiliary loops were measured by means of magnetic flow meters. All the measured values are scanned and recorded every 1 s by a data logger connected to a computer; the data collected over a period of 300 s at steady state conditions were time-averaged to determine the experimental data points.

The uncertainties of all these instruments are reported in Table 2.

More detailed information on the setup of the test circuit, on the test section, the measuring instruments and the test procedure adopted can be found in previous works published by the same authors [13–16].

The experimental data were expressed as a function of average heat transfer coefficient (HTC) and frictional pressure drops. To evaluate the average HTC, the temperature of the tube wall was measured using four T-type thermocouples.

 Table 2
 Specification of the different measuring devices

| Devices | Uncertainty $(k=2)$ | Range |
|-----------------------------|---------------------|---------------------------|
| T-type thermocouples | 0.1 K | −20/80 °C |
| T-type thermopiles | 0.05 K | −20/80 °C |
| Abs. pressure transducers | 0.075% f.s. | 0/3.0 MPa |
| Diff. pressure transducers | 0.075% f.s. | 0/0.3 MPa |
| Coriolis effect flow meters | 0.1% | $0/300 \text{ kg h}^{-1}$ |
| Magnetic flow meters | 0.15% f.s. | $100/1200 \ 1 \ h^{-1}$ |
| Data logger | $\pm~2.7~\mu V$ | $0\:/\:100\:mV$ |

Two thermocouples were inserted 100 mm from the measuring section entrance and the other two 100 mm from the measuring section output. For each pair, one thermocouple was embedded inside a groove and sealed in the upper part of the tube and the other in the lower part of the tube.

In this way it was possible to evaluate the *HTC* according to Eq. 1.

$$HTC = \frac{Q_w}{A \left(t_{wall} - t_{sat} \right)} \tag{1}$$

Where Q_w is obtained from a thermal balance on the heating water loop and t_{sat} is the average saturation temperature evaluated from the average refrigerant

 Table 3
 Experimental campaign testing conditions

| Refrig | erant R600a | | | | |
|--------|-------------|-------------|---------------------------------------|-----------------------|-------------|
| Runs | t_{sat} | p_{sat} | G | q | X |
| | [°C] | [bar] | [kg m ⁻² s ⁻¹] | [kW m ⁻²] | [-] |
| 31 | 20.2-20.0 | 3.045-3.018 | 302-99 | 312-146 | 0.08-0.75 |
| 32 | 10.3-9.9 | 2.237-2.199 | 306-101 | 306-147 | 0.12-0.75 |
| 30 | 5.2-4.8 | 1.195-1.855 | 304-102 | 309-149 | 0.13-0.71 |
| Refrig | erant R152a | | | | |
| Runs | t_{sat} | p_{sat} | G | q | X |
| | [°C] | [bar] | $[kg m^{-2} s^{-1}]$ | $[kW m^{-2}]$ | [-] |
| 34 | 20.0-19.9 | 5.140-5.118 | 404-149 | 310-151 | 0.07 – 0.84 |
| 35 | 15.1-14.9 | 4.404-4.377 | 403-147 | 307-149 | 0.10-0.85 |
| 33 | 10.0-9.9 | 3.736-3.702 | 408-151 | 309-149 | 0.10-0.79 |



Fig. 2 Average *HTC* vs. mean vapor quality during R600a flow boiling at G = 100, 150, 200, and 300 kg m⁻² s⁻¹ and the heat flux q = 20 kW m⁻². Saturation temperature of 20 °C (left), 10 °C (centre) and 5 °C (right)

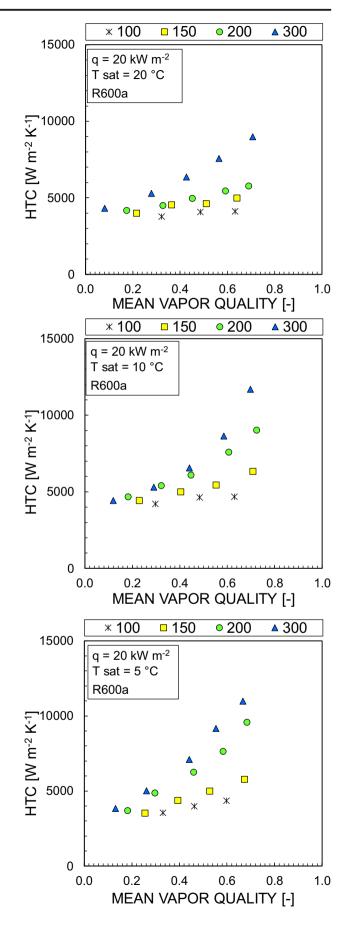




Fig. 3 Average *HTC* vs. mean vapor quality during R600a flow boiling at $q=15, 20, 25, \text{ and } 30 \text{ kW m}^{-2} \text{ and } G=200 \text{ kg m}^{-2} \text{ s}^{-1}$. Saturation temperature of 20 °C (left), 10 °C (centre) and 5 °C (right)

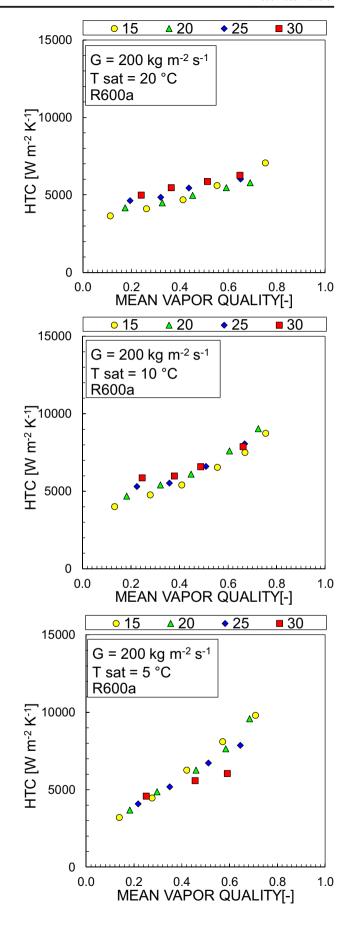




Fig. 4 Frictional pressure drop vs. mean vapor quality during R600a flow boiling at G=100, 150, 200, and 300 kg m⁻² s⁻¹. Saturation temperature of 20 °C (left), 10 °C (centre) and 5 °C (right)

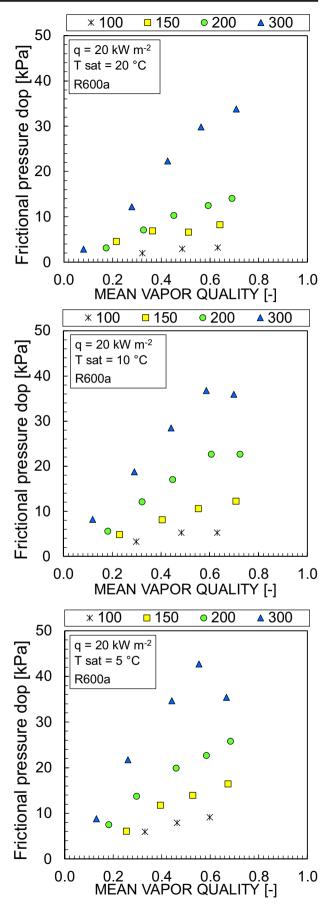




Fig. 5 Average *HTC* vs. mean vapor quality during R152a flow boiling at G = 150, 200, 300, and $400 \text{ kg m}^{-2} \text{ s}^{-1}$ and the heat flux $q = 20 \text{ kW m}^{-2}$. Saturation temperature of 20 °C (left), 15 °C (centre) and 10 °C (right)

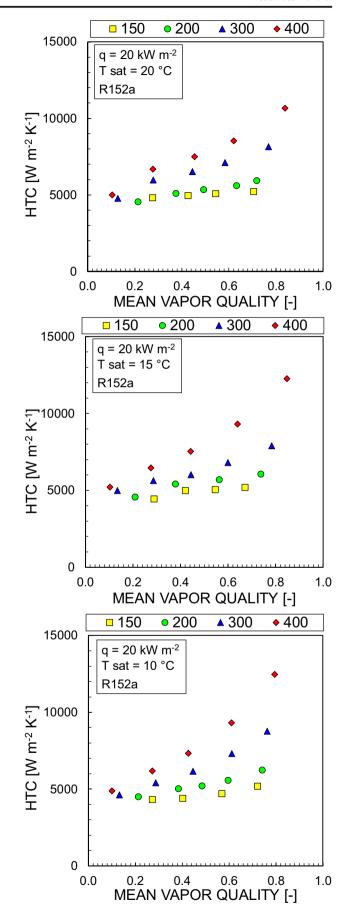




Fig. 6 Average *HTC* vs. mean vapor quality during R152a flow boiling at $q=15, 20, 25, \text{ and } 30 \text{ kW m}^{-2} \text{ and } G=300 \text{ kg m}^{-2} \text{ s}^{-1}$. Saturation temperature of 20 °C (left), 15 °C (centre) and 10 °C (right)

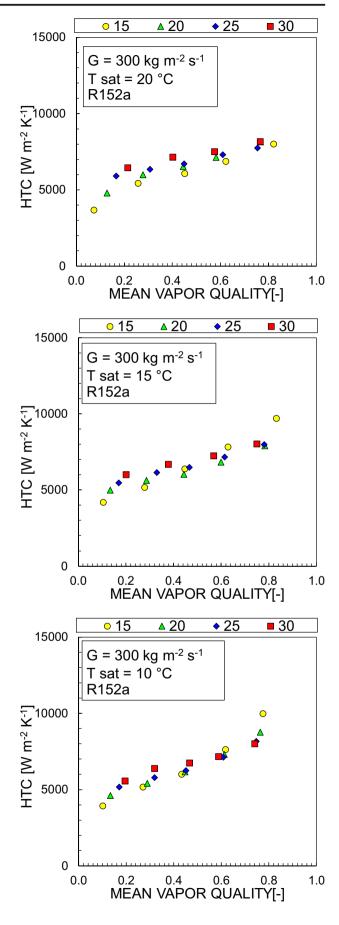




Fig. 7 Frictional pressure drop vs. mean vapor quality during R152a flow boiling at G=150, 200, 300, and 400 kg m $^{-2}$ s $^{-1}$. Saturation temperature of 20 °C (left), 15 °C (centre) and 10 °C (right)

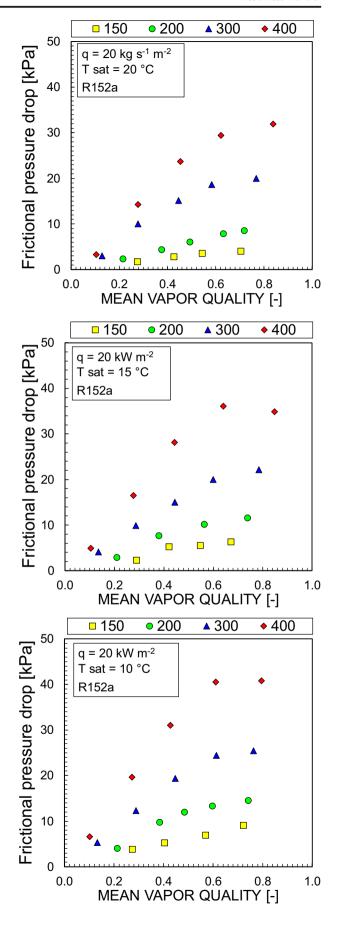




Table 4 Relative and absolute deviations between correlations and experimental *HTC* data

Mean relative deviation (%)

| | R600a | R152a |
|------------------------------------|-------|-------|
| Gungor and Winterton [19] | -5.1 | -9.5 |
| Liu and Winterton [20] | 11.2 | -0.9 |
| Zhang et al. [21] | -17.5 | -15.7 |
| Saitoh et al. [22] | -24.4 | -26.6 |
| Sun and Mishima [23] | -33.4 | -15.9 |
| Oh and Son [24] | -19.6 | -14.5 |
| Kim and Mudawar [25] | -14.9 | -8.7 |
| Fang et al. [26] | -6.2 | 5.1 |
| Sempertegui Tapia and Ribatski [9] | 29.8 | 16.5 |
| Mean absolute deviation (%) | | |
| | R600a | R152a |
| Gungor and Winterton [19] | 19.4 | 15.8 |
| Liu and Winterton [20] | 18.1 | 7.1 |
| Zhang et al. [21] | 22.1 | 15.8 |
| Saitoh et al. [22] | 24.4 | 26.6 |
| Sun and Mishima [23] | 33.4 | 18.2 |
| Oh and Son [24] | 19.9 | 16.0 |
| Kim and Mudawar [25] | 15.1 | 9.6 |
| Fang et al. [26] | 6.2 | 5.1 |
| Sempertegui Tapia and Ribatski [9] | 29.8 | 16.6 |

pressure. Refprop v.10 [17] is used to calculate the refrigerants' thermophysical properties. A thermal balance at the pre-evaporator is used to estimate the vapor quality at the inlet of the test section, as:

$$\dot{m}_{w}c_{p,w}(t_{pre,in}-t_{pre,out}) = \dot{m}_{ref}(J_{in}-J_{sub})$$
 (2)

Where m_w is the water mass flow rate, $c_{p,w}$ is the specific heat capacity of the water, $t_{pre,in}$ and $t_{pre,out}$ are the water

temperatures measured at the inlet and outlet, respectively of the pre-evaporator. \dot{m}_{ref} is the refrigerant mass flow rate and J_{in} the specific enthalpy of the refrigerant at the inlet of the test section while J_{sub} is the specific enthalpy of the refrigerant at the inlet of the pre-evaporator, which is evaluated with Refprop v10 [17] from the measured values of the refrigerant pressure and temperature. The specific enthalpy J_{in} is then used to estimate the inlet vapor quality and with a second thermal balance at the test section it is possible to evaluate the outlet vapor quality and, eventually, the mean value by averaging those two.

Subsequently, pressure drops are also analyzed. The focus was placed on frictional pressure drops which are evaluated according to Eq. 3.

$$\Delta p_f = \Delta p_{tot} - \Delta p_a - \Delta p_c \tag{3}$$

a length between the two pressure taps of 1300 mm is taken into consideration which considers the entire 4 mm tube.

The homogeneous model for the two phase flow is adopted, to be consistent with other data already published and to allow a comparison between them and the new ones [13, 16]. So, the momentum pressure drops are calculated according Eq. 4:

$$\Delta p_a = G^2(\mathbf{v}_G - \mathbf{v}_L)|\Delta \mathbf{x}| \tag{4}$$

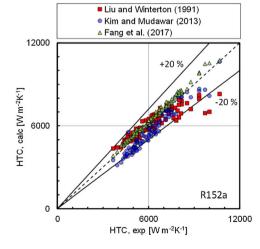
Again, to be consistent to the previous data base of data published, the local pressure drops are are calculated according Eq. 5.

$$\Delta p_c = 1.0 G^2 / (2\rho_{\rm m} \cdot {\rm w}) \tag{5}$$

where the average two phase density is used according to the homogeneous model.

Using the procedure proposed by the Kline and McClintock [18], an uncertainty analysis was carried out on the of *HTC* and frictional pressure drop.

Fig. 8 Calculated vs. experimental average *HTC* obtained with R152a and R600a



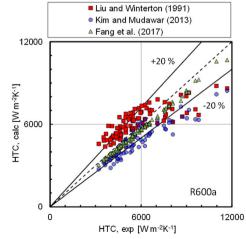




 Table 5
 Relative and absolute deviations between correlations and experimental frictional pressure drops data

Mean relative deviation (%)

| | R600a | R152a |
|---------------------------------|-------|-------|
| Friedel [28] | -4.9 | -7.8 |
| Müller Steinhagen and Heck [29] | -7.9 | -14.5 |
| Mishima and Hibiki [34] | 15.4 | 13.3 |
| Wang et al. [33] | 4.1 | 0.0 |
| Sun and Mishima [23] | 7.5 | -0.4 |
| Kim and Mudawar [32] | -1.2 | -8.4 |
| Mean absolute deviation (%) | | |
| | R600a | R152a |
| Friedel [28] | 19.69 | 23.02 |
| Müller Steinhagen and Heck [29] | 16.28 | 21.14 |
| Mishima and Hibiki [34] | 24.28 | 24.22 |
| Wang et al. [33] | 15.49 | 14.87 |
| Sun and Mishima [23] | 27.74 | 32.18 |
| Kim and Mudawar [32] | 19.89 | 22.03 |

The maximum uncertainty on *HTC* is of 7% and on the friction pressure drop is of 8%.

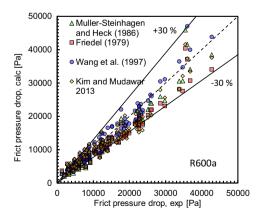
3 Results and discussion

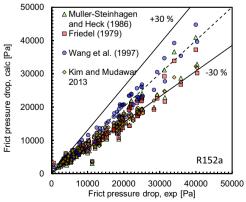
The experimental campaign presented in this work aimed to collect new average heat transfer coefficient and frictional pressure drop data during flow boiling of two refrigerants: R600a and R152a inside the same 4 mm smooth tube.

93 new experimental points were collected using R600a and 102 with R152a. For each refrigerant: three saturation temperatures, four mass velocities, and four heat flux were investigated.

In detail, R600a was studied at 20, 10 and 5 $^{\circ}$ C of saturation temperature. At each temperature, the specific mass flow rates of 100, 150, 200 and 300 kg m $^{-2}$ s $^{-1}$ were taken into consideration. They have been tested maintaining a constant heat flux of 20 kW m $^{-2}$.

Fig. 9 Calculated vs. experimental frictional pressure drops obtained with R152a and R600a





Then, the specific mass flow rate $G = 200 \text{ kg m}^{-2} \text{ s}^{-1}$ was kept constant and four heat fluxes of 15, 20, 25 and 30 kW m^{-2} were investigated.

A similar test campaign was also conducted with R152a as refrigerant. Since its thermophysical properties are different from those of R600a, it was decided to investigate it under different operating conditions.

In any case, three saturation temperatures were studied: 20, 15 and 10 °C.

For each temperature, four specific mass flow rates were taken into account (G = 150, 200, 300, and 400 kg m⁻² s⁻¹) and the heat flux was set at 20 kW m⁻². Finally, at G = 300 kg m⁻² s⁻¹ the same heat fluxes were imposed (q = 15, 20, 25 and 30 kW m⁻²).

In this way, it was possible to separately analyze the effects of the saturation temperature, the heat flux and the mass flow rate on the flow boiling heat transfer.

Table 3 lists the experimental datasets, subdivided by refrigerant and saturation temperature. It also highlights the maximum and minimum values reached in each set of: saturation temperature, saturation pressure, specific mass flow rate, heat flux, and average vapor quality- evaluated as the average value between inlet and outlet vapor quality. The datasets were collected by varying vapor quality.

Each set started with low vapor quality values. Subsequently, the average vapor quality was increased to the point where the dryout phenomenon was observed. This phenomenon is extremely abrupt, and it involves a drastic reduction of *HTC*. It is anticipated by a strong instability of the wall temperatures closed to the outlet of the measuring section.

This article wants to focus on the analysis of average *HTC* before the dryout phenomenon, so the last experimental point of each series was recorded just before the instability on the wall temperatures occurred.

Furthermore, repeatability tests were carried out. In these tests, the data set order was reversed. The data were generated starting from the maximum vapor quality up to the minimum vapor quality. No hysteresis phenomena were observed. All the repeated conditions gave overlapping results within $\pm 2\%$.



Table 6 R134a, R600a, and R152a main thermophysical properties evaluated with Refprop v.10 [17] at 20 °C of saturation temperature

| Parameter | Unit | R134a | R600a | R152a |
|--------------------|-----------------------|--------|--------|---------|
| p _{crit} | [bar] | 40.591 | 36.290 | 45.167 |
| p_{sat} | [bar] | 5.717 | 3.022 | 5.129 |
| p_{red} | [-] | 0.141 | 0.083 | 0.114 |
| $ ho_{L}$ | $[kg m^{-3}]$ | 1225.3 | 556.9 | 912.0 |
| $ ho_{ m V}$ | $[kg m^{-3}]$ | 27.78 | 7.91 | 15.91 |
| c_{pL} | $[J kg^{-1} K^{-1}]$ | 1404.9 | 2398.2 | 1776.5 |
| c_{pV} | $[J kg^{-1} K^{-1}]$ | 1000.7 | 1757.3 | 1217.3 |
| r | $[kJ kg^{-1}]$ | 182.28 | 334.33 | 285.32 |
| k_{L} | $[mW m^{-1} K^{-1}]$ | 83.284 | 91.071 | 100.205 |
| $k_{\rm V}$ | $[mW m^{-1} K^{-1}]$ | 13.335 | 16.292 | 14.240 |
| μ_{L} | $[\mu Pa s^{-1}]$ | 207.37 | 159.34 | 172.76 |
| μ_{V} | $[\mu Pa s^{-1}]$ | 11.49 | 7.37 | 9.88 |
| σ | [mN m ⁻¹] | 8.69 | 10.56 | 10.38 |

3.1 NEW R600a EXPERIMENTAL DATA

Figure 2 reports the average HTC plotted against the mean vapor quality at different mass flow rates (G = 100, 150,

200, and 300 kg $\rm m^{-2}~s^{-1})$ and at the same heat flux of 20 kW $\rm m^{-2}.$

The three charts report data relating to three different saturation temperatures: 20 °C, 10 °C, and 5 °C. At G =100 kg m⁻² s⁻¹, the HTC remains almost constant as a function of the mean vapor quality with values around 4000 W m⁻² K⁻¹. Under these conditions, the convective effects are likely to be negligible, in fact, the HTC is not affected by the variation in vapor quality. On the other hand, in the case of high mass flow rates, HTC grows considerably (up to 2.5 times, when $G = 300 \text{ kg m}^{-2} \text{ s}^{-1}$ is investigated) as a function of the vapor quality. Under these conditions, it is very probable that the heat transfer is more affected by convective mechanisms as compared to the nucleate boiling. They become more intense at high flow rates, high vapor qualities and low saturation pressures (Kim and Mudawar [19]). The experimental data obtained reflect precisely what stated by the theory.

For these reasons, at low vapor quality, the HTC changes very little when passing from one mass flow rate to another. Instead at high vapor qualities, the HTC increases significantly with the increase in the mass flow rate (up to +160% from $G = 100 \text{ kg m}^{-2} \text{ s}^{-1}$ to $G = 300 \text{ kg m}^{-2} \text{ s}^{-1}$ at x = 0.75).

Fig. 10 Comparison between R134a, R600a and R152a heat transfer coefficients at the same working conditions

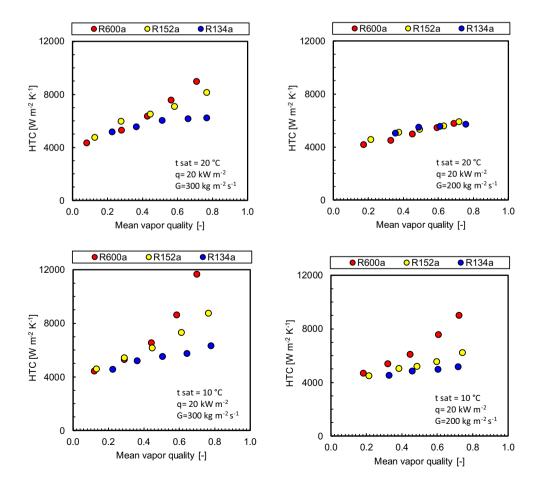




Fig. 11 Comparison between R134a, R600a and R152a frictional pressure drops at the same working conditions

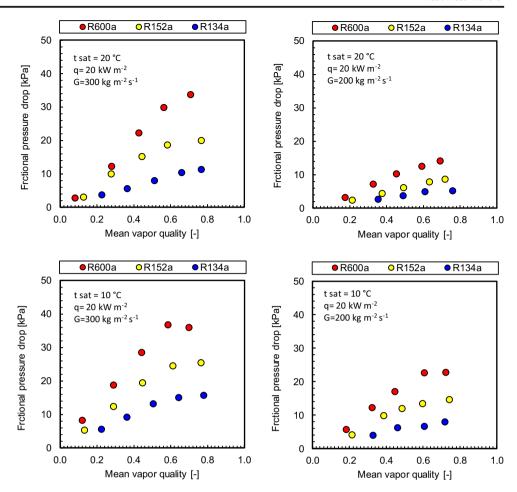


Fig. 3 reports the average HTC plotted against the mean vapor quality at different heat fluxes (q = 10, 15, 20, and 30 kW m⁻²) and at the same mass flow rate of 300 kg m⁻² s⁻¹.

Again, the three charts report data relating to three different saturation temperatures: 20 °C, 10 °C, and 5 °C.

Contrary to what was observed when the mass flux changes (see Fig. 2), when the heat flux changes (Fig. 3), at the same vapor quality there is a reduced variation of HTC (up to +20%, but on average + 15%). Then, HTC tends to grow with increasing vapor quality (up to +320% at $q = 15 \text{ kW m}^{-2}$ and $t_{sat} = 5$ °C). This increase is more significant at low saturation temperatures (the increase is more than 200% at $t_{sat} = 5$ °C, while is slightly lower than 100% at $t_{sat} = 20$ °C). In fact, a low pressure enhances the convective mechanisms that lead to increase the heat transfer. Furthermore, it can be noted that HTC's sensitivity to the increase in vapor quality is more noticeable at low heat flux because, at these operating conditions, the convective boiling is stronger. This behavior was also observed and theorized by Kim and Mudawar [19] in their comprehensive review of the underlying heat transfer mechanisms during flow boiling.

Figure 4 reports three charts, one for each saturation temperature (20, 10, and 5 $^{\circ}$ C) where the frictional pressure drops

are plotted against the mean vapor quality at different mass flow rates ($G = 100, 150, 200, \text{ and } 300 \text{ kg m}^{-2} \text{ s}^{-1}$).

As expected, frictional pressure drops increase as the mass flow rate increases. Furthermore, they also increase with an increase in vapor quality. At very high vapor qualities they begin to decrease because they are going to reach the value they would have in case of only vapor flow.

The frictional pressure drop measurements are not affected by the heat flux variation. For this reason, the related graphs are here reported.

3.2 NEW R152a EXPERIMENTAL DATA

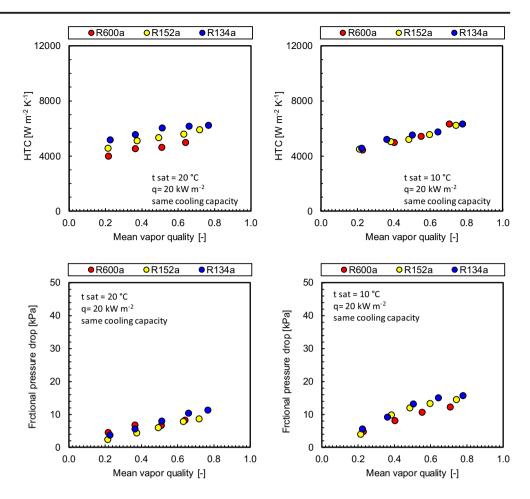
In this paragraph the experimental results obtained with R152a are reported. Figure 5 shows the average HTC values plotted against the mean vapor quality at different mass flow rates (in this case $G = 150, 200, 300, \text{ and } 400 \text{ kg m}^{-2} \text{ s}^{-1}$) and at the same heat flux of 20 kW m⁻².

When R152a was studied, three different saturation temperatures were investigated: 20 $^{\circ}$ C, 15 $^{\circ}$ C, and 10 $^{\circ}$ C. The three charts are related to these temperatures.

At a first glance, in the present range of operating conditions, the trend of the graphs obtained with R152a is very



Fig. 12 Comparison between R134a, R600a and R152a heat transfer coefficients and frictional pressure drops at the same cooling capacity



similar to that observed with R600a. Again, it is possible to notice an increase in HTC as the mass flow rate increases (+130%). Furthermore, the HTC remains almost constant in function of the vapor quality at low mass flow rates (HTC increases up to +15% at $G=150~kg~m^{-2}~s^{-1}$). On the other hand, when the investigated mass flow rate is high, HTC is strongly dependent on vapor quality (HTC increases up to +140% at $G=400~kg~m^{-2}~s^{-1}$). These evidences confirm that the two competing heat transfer mechanisms: nucleate boiling and convective flow boiling seem to behave as expected and as it was observed for R152a.

Figure 6 reports the same information shown in Fig. 3, but in this case the data refers to R152a. The average HTC is plotted against the mean vapor quality at a constant mass flow rate of 300 kg m⁻² s⁻¹ and at four heat fluxes (15, 20, 25, and 30 kW m⁻²).

Again, HTC's tendency is to slightly increase as a function of heat flux (up to +70% at lower vapor qualities, but on average + 18%). Furthermore, it increases when increasing vapor quality, especially in the datasets obtained at lower heat flux (+150% at $q = 15 \text{ kW m}^{-2}$ and $t_{\text{sat}} = 10 \,^{\circ}\text{C}$). Finally, Fig. 7 plots the frictional pressure drops exhibited by R152a flowing in the 1300 mm long tube. The frictional pressure drops are plotted against the mean vapor quality at different mass flow

rates (G = 150, 200, 300, and 400 kg m⁻² s⁻¹). Again, the saturation temperatures of 20, 15, and 10 °C are investigated.

Also in this case, the experimental trend obtained reflects what was expected. Frictional pressure drops increase with increasing mass flow rate and average vapor quality.

3.3 Models assessment

To confirm the quality of the experimental data obtained, it was chosen to compare the values of HTC and frictional pressure drop against several correlations present in the open literature. The investigated tube has a diameter of 4 mm, hence it can be considered a "small" or "compact" tube since its diameter is of small size for being a standard tube, but large for being a mini-channel. There are not many experimental data collected in channels having such a hydraulic diameter. For this reason, it is quite difficult to find correlations developed with a databank containing many 4 mm diameter data. It was chosen to consider classical correlations, which are universally recognized to be reliable for the estimation of heat transfer coefficient during flow boiling inside tube. Among these, the correlation proposed by Gungor and Winterton [19] which was developed on 3693 data, mainly of water and other refrigerants used at the time like R11 and R12, in



tubes with diameters between 2.95 mm and 32 mm. In any case, the bulk of the data was collected in tubes with a diameter between 15 and 20 mm. The Liu and Winterton correlation [20] was also taken into consideration. It is based on a database of 4202 data generated by flow boiling in tubes having diameters between 3 and 32 mm. Once again, data are obtained from water flow boiling and numerous refrigerants present at the time like R12 and R22. Subsequently, the correlation of Zhang et al. [21] has been investigated. It focuses on data collected with small diameter tubes, ranging between 0.7 mm and 3.1 mm. Once again there are data of water and refrigerants now phased off, such as R11, R12, and R113.

More recent is the model of Saitoh et al. [22] which proposes a modified Chen-type correlation based on a databank containing also data collected with R134a and 3.1 mm diameter tubes.

The Sun and Mishima model [23] used a database of 2505 data obtained in tubes with a diameter between 0.21 mm and 6.5 mm, among which there are R134a data.

R134a flow boiling data are also present in the Oh and Son correlation [24], in this case inside a 3.36 mm diameter tube.

Even more recent is the correlation proposed by Kim and Mudawar [25]. It is based on a very large database of experimental tests carried out in channels having diameters between 0.3 mm and 6 mm. In this case there are also 45 data of R152a which flows in a 1 mm diameter tube by Hamdar et al. [7].

Finally, the correlation of Sempertegui Tapia and Ribatski [6] contains 1315 data of R600a within the database of 3409 data used to generate it. These data were collected by the same authors in a small diameter tube (1.1 mm) at relatively high saturation temperatures (31 °C and 41 °C).

Finally, the model by Fang et al. [26] was included. This equation is fitted on a very large database, including R600a data of Yang et al. [4] and the R152a data of Hamdar et al. [7]. Fang and his group, in their review [1] tested several models and found that the Fang et al. [26] equation used for R134a, R600a and R152a outperformed any other equation considered by them. It is worth to underline that they included, among others, all the models considered in the present paper with the only exceptions of Sempertegui Tapia and Ribatski [6] and Oh and Son [25] models.

Table 4 reports the mean relative deviation and the mean absolute deviation between the results calculated by the correlations listed above in chronological order and the *HTC* experimental data presented in this article.

The models with a lower absolute deviation are Fang et al. [26], Liu and Winterton [20] and Kim and Mudawar [25].

All the three models were generated based on a very large database, both in terms of number of data, of hydraulic diameters investigated and of refrigerants used.

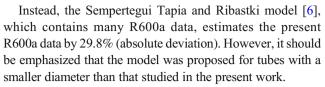


Figure 8 finally shows two graphs plotting the *HTC* calculated with the correlations of Fang et al. [26], Kim and Mudawar [25] and Liu and Winterton [20] (the three best correlations) and the experimental data. The correlation of Fang et al. [26] is able to well predict both the trend and the values of the experimental data.

Regarding pressure drops, the number of data sets available in the literature for R600a and R152a is rather limited, as presented in Table 1.

Copetti et al. [3] observed that the frictional pressure drops measurements carried out with R600a showed quite large deviations from results obtained by usual correlations. Qiu et al. [5] observed that the Grönnerud model [27] was the unique method capable to properly capture their isobutane pressure drop measurements, while classical models like Friedel [28] and Müller Steinhagen and Heck [29] did not perform acceptably. Differently, Yang et al. [4] found an acceptable consistency of their data with Müller Steinhagen and Heck [29]. Similar results were found by Hamdar and co-authors [7] for their R152a measurements. Sempertegui Tapia and Ribatski [30] observed that Del Col et al. [31] model outperformed both the Müller Steinhagen and Heck [29] and the Friedel [28] model in the estimation of their R600a pressure drop measurements.

For this reason, in the present research, it was decided to implement six correlations.

The one proposed by Kim and Mudawar [32] is the most recent and it is based on a very extensive databank of 2378 data, mostly obtained with R134a flowing in tubes having a hydraulic diameter between 0.3 and 5.3 mm.

Also the correlations of Sun and Mishima [23] and Wang et al. [33] were developed with some R134a data. The first one contains data in tube with a diameter from 0.2 mm to 6.5 mm, while the second one R134a was flowing in a round rube having a diameter of 6.5 mm.

In addition, more classic correlations have been tested, such as Mishima and Hibiki [34], Friedel [28], and Müller-Steinhagen and Heck [29]. The last two equations were implemented and tested on very large databases, however they have been developed on other groups of refrigerants that were present at the time, now phased out. Mishima and Hibiki [34] was finally developed on water-air two-phase flow in vertical small tube.

Table 5 shows mean relative deviation and mean absolute deviation between these frictional pressure drop correlations listed in chronological order and the experimental data.

The correlation that presents the lowest absolute deviation was the Wang et al. [33] (15.9% and 14.9% for R600a and



R152a data respectively) followed by the Kim and Mudawar [32], the Müller Steinhagen and Heck [29] and the Friedel [28] ones.

In addition, to give a direct and clear information about the best four correlations, the estimated values are plotted against the experimental frictional pressure drops of R600a and R152a in Fig. 9.

3.4 Refrigerants comparison

The main purpose of these experimental tests is to expand the literature database, by adding heat transfer and pressure drop data of refrigerants that may be used to replace R134a.

In fact, the issue of the phase out of R134a is still very urgent. R134a is probably one of the most widespread refrigerants in the past twenty years. It has been used in the most varied areas of refrigeration: domestic refrigeration, automotive, large chillers, air conditioning. For this reason it is essential to find environmentally friendly alternatives that can replace it. Table 6 lists the main thermophysical properties of R134a, R600a, and R152a evaluated with Refprop v.10 [17] at 20 °C of saturation temperature.

R152a and R134a exhibit a similar saturation pressure, while R600a has a saturation pressure about half of R134a one.

R134a has the highest reduced pressure. R152a has a reduced pressure 20% lower, while R600a has it around 40% lower than R134a.

R134a has also the highest liquid and vapor densities, while R600a has the lowest (-55% for liquid and -72% for vapor).

Another property that is different among the three refrigerants is the latent heat. In this case, R600a has the highest, almost double that of R134a. R152a has a latent heat 50% greater than that of R134a.

Thermal conductivity, on the other hand, is similar between the three refrigerants. R152a has a liquid thermal conductivity 20% greater than that of R134a, while the R600a one is about 10% greater than that of R134a.

The different thermophysical properties cause a different heat transfer behavior. Several theoretical or semi-empirical approaches can be used as reported for example in Longo et al. [35] in order to properly rank the fluids heat transfer performance by coupling their heat transfer coefficient to their saturation temperature drop that is linked to their pressure drops. This comprehensive approach goes beyond the scope of the present paper. Here we prefer to compare the original experimental points previously presented with some experimental measurements obtained with R134a in the same rig and already presented in [14].

Figure 10 presents a comparison between R134a, R600a and R152a HTC at the same working conditions. They are: heat flux $q = 20 \text{ kW m}^{-2}$, $G = 300 \text{ and } 200 \text{ kg m}^{-2} \text{ s}^{-1}$, and saturation temperatures 20 and 10 °C.

The first graph shows $G = 300 \text{ kg m}^{-2} \text{ s}^{-1}$ and $t_{sat} = 20 \text{ °C}$. At low vapor qualities the three refrigerants have similar performances. The HTC of R600a, however, is more affected by the convective contribution and it increases more significantly with the increase in vapor quality (moving from the minimum to the maximum vapor quality, R600a HTC increases of about +110%, while R134a one of about +20%). For this reason, at high vapor qualities R600a outperforms the

The convective mechanism is reinforced by the lower reduced pressure of R600a and also by the lower vapor density.

other refrigerants (HTC about 45% higher than R134a).

Instead, when the refrigerants are compared at lower mass velocity (see the second graph where $G = 200 \text{ kg m}^{-2} \text{ s}^{-1}$) the convective mechanism is less relevant and it gives a lower contribute to the increase of the *HTC*. For this reason, the performances of the three refrigerants are equivalent.

A decrease in saturation temperatures strengthens the contribution of convective heat transfer. The third and the fourth graphs of Fig. 10 are collected at 10 °C of saturation temperature.

R600a is the fluid mostly influenced by the reduction in saturation temperature, due to its lower saturation pressure and reduced pressure. For this reason, it is mainly affected by the increase in the convective contribution, and it outperforms other refrigerants at high vapor qualities (+75% with respect to R134a).

For the same reason, R134a is the refrigerant that has the lowest *HTC*, among the three investigated.

The reduced pressure also has a great influence on pressure drops. Fig. 11 presents the frictional pressure drops at the same working conditions illustrated in Fig. 10.

In this case, higher reduced pressure leads to lower pressure drops. And for this reason, R134a has the lowest pressure drops among the refrigerants in all conditions (up to 3 times lower at high vapor qualities and high mass velocities).

Since two alternative refrigerants are proposed to replace R134a within refrigeration systems, it can be interesting to compare the three fluids having as the objective "the same cooling capacity", that is defined as the product of latent heat and mass flow rate. Consequently, to have an equal cooling capacity, for a given vapor quality change and keeping as a reference the needed mass flow rate of the R134a, the mass flow rate of R600a must be almost half while that of R152a must be around 40% lower of that R134a one. Thus, considering the whole latent heat (i.e. a vapor quality change of 1), it is possible to run a rationale comparison between the three refrigerants.

Figure 12 presents a comparison between refrigerants with the same cooling capacity, at two saturation temperatures: $20 \, ^{\circ}\text{C}$ and $10 \, ^{\circ}\text{C}$ both in terms of HTC and frictional pressure drops.

In this case, the performances of the three refrigerants are very similar to each other. R134a slightly outperforms the



other two fluids at 20 $^{\circ}$ C of saturation temperature, but at 10 $^{\circ}$ C the performances are superimposable. The same conclusions can be drawn by analyzing the respective frictional pressure drops.

As demonstrated with the experimental tests presented in this paper, during the flow boiling process within a round rube it is possible to say that both R600a and R152a are potentially good substitutes for R134a. It remains up to the designer to be able to exploit the characteristics and capabilities of each refrigerant.

4 Conclusions

This article presented 93 new R600a data points and 102 new R152a data points during flow boiling inside at 4 mm ID horizontal round tube.

Saturation temperatures of 10, 15, 10, and 5 $^{\circ}$ C were investigated, the mass flux ranged between 100 and 300 kg m $^{-2}$ s $^{-1}$ and the heat flux between 15 and 30 kW m $^{-2}$.

In the first part of the paper, all the collected experimental data were presented in terms of average heat transfer coefficient and frictional pressure drop.

For both refrigerants, it was observed that the heat transfer coefficient remarkably increased with the increase of the mass flux while it slightly increased with the heat flux.

Then, it was noted that under some working conditions, the heat transfer coefficient is more affected by the convective mechanism. In fact, it enhances the heat transfer coefficient at low saturation temperatures, high mass fluxes, low heat fluxes, and high vapor qualities.

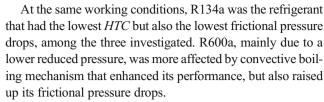
As expected, frictional pressure drops increased as the increasing of the mass flow rate, while they were not affected by the heat flux variation.

Following, several heat transfer coefficient and frictional pressure drop correlations were assessed against the experimental data.

The heat transfer coefficient models by Fang et al. [26], Liu and Winterton [20] and Kim and Mudawar [25] presented the lowest mean absolute deviations for R152a and R600a, but it was the Fang et al. model [26] that better captured the data trend.

The frictional pressure drops correlation that presented the lowest absolute deviation was the Wang et al. [33] (15.9% and 14.9 for R600a and R152a data respectively) followed by the Kim and Mudawar [32], the Müller Steinhagen and Heck 291] and the Friedel [28] ones.

Finally, the heat transfer performance of R600a and R152a were compared against that of R134a. In fact, the issue of the R134a phase-out is still very urgent, and there is a strong need to find out valid low GWP alternatives to R134a. The experimental data were compared at the same mass flux and heat flux, and at the same cooling capacity.



When the same cooling capacity was considered, the performances of the three refrigerants were very similar to each other.

So, it is possible to conclude that during flow boiling heat transfer inside a compact smooth circular tube both R600a and R152a are potentially good substitutes for R134a. It remains up to the designer to be able to exploit the characteristics and capabilities of each refrigerant.

Acknowledgements This research work was partly funded by the ZeroGWP Project LIFE17 CCM/IT/000026 and by the PRIN 2017 FlexHeat 2017KAAECT project.

Funding Open access funding provided by Università degli Studi di Padova within the CRUI-CARE Agreement.

Compliance with ethical standards

Conflict of interest On behalf of all authors, the corresponding author states that there is no conflict of interest.

Open Access This article is licensed under a Creative Commons Attribution 4.0 International License, which permits use, sharing, adaptation, distribution and reproduction in any medium or format, as long as you give appropriate credit to the original author(s) and the source, provide a link to the Creative Commons licence, and indicate if changes were made. The images or other third party material in this article are included in the article's Creative Commons licence, unless indicated otherwise in a credit line to the material. If material is not included in the article's Creative Commons licence and your intended use is not permitted by statutory regulation or exceeds the permitted use, you will need to obtain permission directly from the copyright holder. To view a copy of this licence, visit hiip://creativecommons.org/licenses/by/4.0/.

References

- Mota-Babiloni A, Navarro-Esbrí J, Molés F, Barragán Cervera Á, Peris B, Verdú G (2016) A review of refrigerant R1234ze(E) recent investigations. Appl Therm Eng 95:211–222
- Harby K (2017) Hydrocarbons and their mixtures as alternatives to environmental unfriendly halogenated refrigerants: an updated overview. Renew Sust Energ Rev 73:1247–1264
- Righetti G, Zilio C, Mancin S, Longo GA (2016) A review on intube two-phase heat transfer of hydro-fluoro-olefines refrigerants. Sci Technol Built Environ 22(8):1191–1225
- Fang X, Zhuang F, Chen C, Wu Q, Chen Y, Chen Y, He Y (2019) Saturated flow boiling heat transfer: review and assessment of prediction methods. Heat Mass Transf 55:197–222
- De Oliveira JD, Copetti JB, Passos JC (2016) An experimental investigation on flow boiling heat transfer of R-600a in a horizontal small tube. Int J Refrig 72:97–110



- Copetti JB, Macagnan MH, Zinani F (2013) Experimental study on R- 600a boiling in 2.6 mm tube. Int J Refrig 36:325–334
- Yang Z, Gong M, Chen G, Zou X, Shen J (2017) Two-phase flow patterns, heat transfer and pressure drop characteristics of R600a during flow boiling inside a horizontal tube. Appl Therm Eng 120: 654–671
- Qiu J, Zhang H, Yu X, Qi Y, Lou J, Wang X (2015) Experimental investigation of flow boiling heat transfer and pressure drops characteristic of R1234ze(E), R600a, and a mixture of R1234ze(E)/R32 in a horizontal smooth tube. Adv Mech Eng 7:1–12
- Sempértegui-Tapia DF, Ribatski G (2017) Flow boiling heat transfer of R134a and low GWP refrigerants in a horizontal micro-scale channel. Int J Heat Mass Transf 108:2417–2432
- Hamdar M, Zoughaib A, Clodic D (2010) Flow boiling heat transfer and pressure drop of pure HFC-152a in a horizontal mini-channel. Int J Refrig 33:566–577
- Anwar Z, Palm B, Khodabandeh R (2014) Flow boiling heat transfer and dryout characteristics of R152ain a vertical mini-channel. Exp Thermal Fluid Sci 53:207–217
- Ross HD (1986) An investigation of horizontal flow boiling of pure and mixed refrigerants, NSBIR 86-3450 report U.S. Department of Commerce. National Bureau of Standards, Gaithersburg, MD
- Longo GA, Mancin S, Righetti G, Zilio C (2019) R1234yf and R1234ze(E) as environmentally friendly replacements of R134a: assessing flow boiling on an experimental basis. Int J Refrig 108: 336–346
- Longo GA, Mancin S, Righetti G, Zilio C (2016) Saturated flow boiling of HFC134a and its low GWP substitute HFO1234ze(E) inside a 4 mm horizontal smooth tube. Int J Refrig 64:32–39
- Longo GA, Mancin S, Righetti G, Zilio C (2017) Hydrocarbon refrigerants HC290 (propane) and HC1270 (propylene) low GWP long-term substitutes for HFC404A: a comparative analysis in vaporisation inside a small-diameter horizontal smooth tube. Appl Therm Eng 124:707–715
- Longo GA, Mancin S, Righetti G, Zilio C (2016) HFC32 and HFC410A flow boiling inside a 4 mm horizontal smooth tube. Int J Refrig 61:12–22
- Lemmon EW, Bell IH, Huber ML, McLinden MO (2018) NIST reference fluid thermodynamic and transport properties database -REFPROP, version 10.0. National Institute of Standards and Technology, Standard Reference Data Program, Gaithersburg
- Kline SJ, McClintock FA (1953) Describing uncertainties in singlesample experiments. Mech Eng 75:3–8
- Gungor KE, Winterton RHS (1986) A general correlation for flow boiling in tubes and annuli. Int J Heat Mass Transf 29(3):351–358
- Liu Z, Winterton RHS (1991) A general correlation for saturated and subcooled flow boiling in tubes and annuli, based on a nucleate pool boiling equation. Int J Heat Mass Transf 34:2759–2766
- Zhang W, Hibiki T, Mishima K (2004) Correlation for flow boiling heat transfer in mini-channels. Int J Heat Mass Transf 47:5749– 5763

- Saitoh S, Daiguji H, Hihara E (2007) Correlation for boiling heat transfer of R-134a in horizontal tubes including effect of tube diameter. Int J Heat Mass Transf 50:5215–5225
- Sun L, Mishima K (2009) An evaluation of prediction methods for saturated flow boiling heat transfer in mini-channels. Int J Heat Mass Transf 52:5323–5329
- Oh HK, Son CH (2011) Flow boiling heat transfer and pressure drop characteristics of CO2 in horizontal tube of 4.57-mm inner diameter. Appl Therm Eng 31:163–172
- Kim SM, Mudawar I (2013) Universal approach to predicting saturated flow boiling heat transfer in mini/micro-channels – part II. Two-phase heat transfer coefficient, Int. J. Heat Mass Transf 64: 1239–1256
- Fang X, Wu Q, Yuan Y (2017) A general correlation for saturated flow boiling heat transfer in channels of various sizes and flow directions. Int J Heat Mass Transf 107:972–981
- 27. Grönnerud R (1979) Investigation of liquid hold-up, flow-resistance and heat transfer in circulation type evaporators, part IV: two-phase flow resistance in boiling refrigerants. Bull de l'Inst du Froid Annexe 1972–1
- Friedel L (1979) Improved friction pressure drop correlations for horizontal and vertical two-phase pipe flow, European two-phase group meeting. Paper E2, Ispra
- Müller-Steinhagen H, Heck K (1986) A simple friction pressure drop correlation for two-phase flow in pipes Chem. Eng Prog 20: 297–308
- Sempértegui-Tapia DF, Ribatski G (2017) Two-phase frictional pressure drop in horizontal micro-scale channels: experimental data analysis and prediction method development. Int J Refrig 79:143– 163
- Del Col D, Bisetto A, Bortolato M, Torresin D, Rossetto L (2013)
 Experiments and updated model for two phase frictional pressure drop inside minichannels. Int J Heat Mass Transf 67:326–337
- Kim SM, Mudawar I (2014) Review of databases and predictive methods for pressure drop in adiabatic, condensing and boiling mini/micro-channel flows. Int J Heat Mass Transf 77:74–97
- Wang CC, Chiang CS, Lu DC (1997) Visual observation of twophase flow pattern of R-22, R-134a, and R-407C in a 6.5-mm smooth tube. Exp Thermal Fluid Sci 15:395–405
- Mishima K, Hibiki T (1996) Some characteristics of air-water twophase flow in small diameter vertical tubes. Int J Multiphs Flow 22: 703–712
- Longo GA, Mancin S, Righetti G, Zilio C, Brown SJ (2020)
 Assessment and optimisation of low-GWP refrigerants during two-phase heat transfer inside small-diameter smooth tubes. Int J Refrig 117:61–70

Publisher's note Springer Nature remains neutral with regard to jurisdictional claims in published maps and institutional affiliations.

